Received: 3 September 2018 | Revised: 9 October 2018 | Accepted: 14 October 2018

DOI: 10.1002/aoc.4686

FULL PAPER

WILEY Applied Organometallic Chemistry

Synthesis of a highly active amino-functionalized Fe_3O_4@SiO_2/APTS/Ru magnetic nanocomposite catalyst for hydrogenation reactions

Yue Liu[1] | Mingxin Lv[1] | Lu Li[3] | Hailong Yu[1] | Qiong Wu[1] | Jinhui Pang[3] | Yuxiang Liu[1] | Congxia Xie[2] | Shitao Yu[1] | Shiwei Liu[1]

[1] College of Chemical Engineering, Qingdao University of Science and Technology, 53 Zhengzhou Road, Qingdao 266042, People's Republic of China

[2] State Key Laboratory Base of Eco-chemical Engineering, College of Chemistry and Molecular Engineering, Qingdao University of Science and Technology, 53 Zhengzhou Road, Qingdao 266042, People's Republic of China

[3] College of Marine Science and Biological Engineering, Qingdao University of Science and Technology, 53 Zhengzhou Road, Qingdao 266042, People's Republic of China

Correspondence
Shitao Yu and Shiwei Liu, College of Chemical Engineering, Qingdao University of Science and Technology, 53 Zhengzhou Road, Qingdao 266042, People's Republic of China.
Email: yushitaoqust@126.com; liushiweiqust@126.com

Funding information
Key R&D project of Shandong; Open Fund of the Biomass-energy and Materials Key Laboratory of Jiangsu, Grant/Award Number: JSBEM201802; National Natural Science Foundation of China, Grant/Award Number: 31700517; Taishan Scholars Projects of Shandong, Grant/Award Numbers: 2017GGX70102 and ts201511033

An amino-functionalized silica-coated Fe_3O_4 nanocomposite (Fe_3O_4@SiO_2/APTS) was synthesized. The Fe_3O_4@SiO_2 microspheres possessed a well-defined core–shell structure, uniform sizes and high magnetization. An immobilized ruthenium nanoparticle catalyst (Fe_3O_4@SiO_2/APTS/Ru) was obtained after coordination and reduction of Ru^{3+} on the Fe_3O_4@SiO_2/APTS nanocomposite. The Ru nanoparticles were not only ultra-small with nearly monodisperse sizes but also had strong affinity with the surface of Fe_3O_4@SiO_2/APTS. The obtained catalyst exhibited excellent catalytic performance for the hydrogenation of a variety of aromatic nitro compounds, even at room temperature. Moreover, Fe_3O_4@SiO_2/APTS/Ru was easily recovered using a magnetic field and directly reused for at least five cycles without significant loss of its activity.

KEYWORDS
amino-functionalized, core–shell structure, Fe_3O_4@SiO_2/APTS/Ru, hydrogenation

1 | INTRODUCTION

Noble metal nanoparticles have shown remarkable potential for numerous applications in electronic, chemical, biological and catalytic fields due to their robustness, ready availability and high surface area properties.[1–3] The larger exposed surface area of the active component of a nanoparticle catalyst enhances markedly the contact between reactants and catalyst and mimics homogeneous catalysts.[4,5] However, owing to their high surface

energies, metallic nanoparticles are normally unstable and tend to coagulate upon sintering during catalytic reactions.[6,7] In order to overcome these problems, extensive studies have been performed to immobilize noble metal nanoparticle catalysts. Numerous methods have been developed to immobilize metal nanoparticles on a large variety of solid supports, such as microporous polymers,[8] mesoporous silica,[9] amorphous silica[10] and carbon nanofibers.[11] However, these methods suffer from tedious and high-cost separation via centrifugation or filtering.

More recently, magnetic core–shell nanocomposites have been widely used as supports for metal nanoparticles.[12–14] Composites with magnetic cores and functional shell structures have received particular attention because the magnetic cores allow the composites to be conveniently collected or separated using an external magnet.[15–18] Functional shells, such as SiO_2 and C, can be applied to immobilize metal nanoparticles.[19] Our team synthesized dense carbon shells embedded in Fe_3O_4 spheres through the hydrothermal treatment of glucose. However, we found that the Fe_3O_4@C microspheres tend to aggregate during the preparation process. Silica has been mostly used as a coating material because it can efficiently inhibit hydrogen ions from passing through.[20] However, silica shells have few functional groups for immobilizing metal nanoparticles on their surface and must be functionalized before being used as supports.[21] Significant attention has been focused on amino functionalization, because amino groups are well known to stabilize metal nanoparticles against aggregation during catalytic reactions.[22] (3-Aminopropyl)triethoxysilane (APTS) has been grafted on the surface of silica shells, where the amino groups of APTS can act as robust stabilizers for supporting metal nanoparticles, thus increasing reusability.[23] Amino-functionalized Fe_3O_4@SiO_2 shows excellent catalytic activity in the selective oxidation of alcohols and the Suzuki reaction.[24,25] Ruthenium-based catalysts have attracted much attention owing to their versatile roles in many catalytic reactions, including the hydrogenation of levulinic acid,[26] CO_2 hydrogenation to formic acid,[27] oxidation of methanol[28] and CO_2 methanation.[29]

Herein, we report the synthesis of a magnetic, amine-functionalized catalyst using APTS as the modifying reagent to immobilize Ru nanoparticles (S1, Scheme 1). Ru nanoparticles are not only ultra-small with nearly monodisperse sizes but also have a strong affinity with the surface of amino-functionalized Fe_3O_4@SiO_2. Fe_3O_4@SiO_2/APTS/Ru exhibits excellent catalytic performance for the hydrogenation of a variety of aromatic nitro compounds, even at room temperature. When the reaction is completed, through a simple magnetic separation, the core–shell Fe_3O_4@SiO_2/APTS/Ru nanocatalyst can be easily recovered with a magnetic field and reused at least five times without significant reduction of catalytic performance.

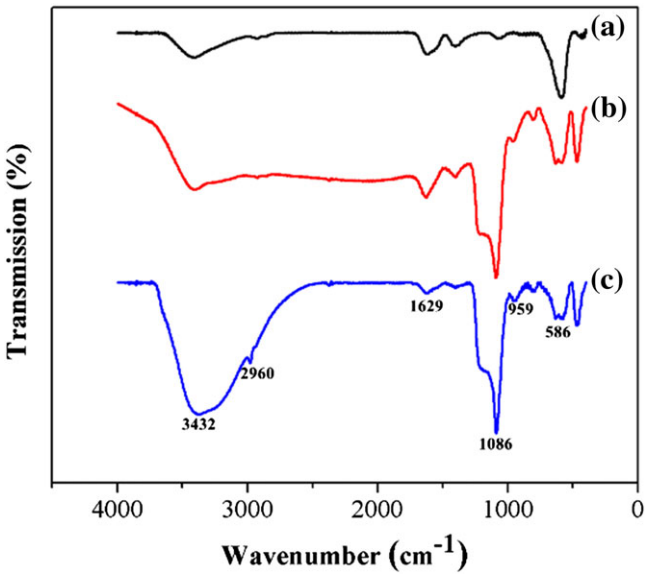

FIGURE 1 FT-IR spectra of Fe_3O_4 (a), Fe_3O_4@SiO_2 (b) and Fe_3O_4@SiO_2/APTS/Ru (c)

2 | RESULTS AND DISCUSSION

2.1 | Structural characterization of Fe_3O_4@SiO_2 and Fe_3O_4@SiO_2/APTS/Ru microspheres

Figure 1 shows the Fourier transform infrared (FT-IR) spectra of the various as-prepared magnetic particles. The absorption band at 586 cm^{-1} in Figure 1a is ascribed to Fe—O—Fe vibrations, which also confirms the presence of Fe_3O_4. In comparison with Figure 1a, the sharp peak at 1086 cm^{-1} in Figure 1b can be assigned to the Si—O—Si vibrations, whereas the peaks at *ca* 1629 and 3432 cm^{-1} are attributed to the absorbed water and hydroxyl groups, respectively. The Si—O bending vibration mode of the silanol group is seen at 959 cm^{-1}. After modification with APTS (Figure 1c), the peaks observed at 2960 cm^{-1} can be

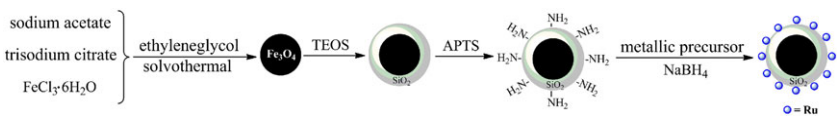

SCHEME 1 Synthesis route to Fe_3O_4@SiO_2/APTS/Ru nanospheres

assigned to the C—H bonds from the silane APTS. Contributions from the —NH_2 group were probably overlapped with vibration bands related to silanol groups and adsorbed water.[30] This result suggests that the surface modification of the Fe_3O_4@SiO_2 core–shell nanospheres was successfully accomplished.

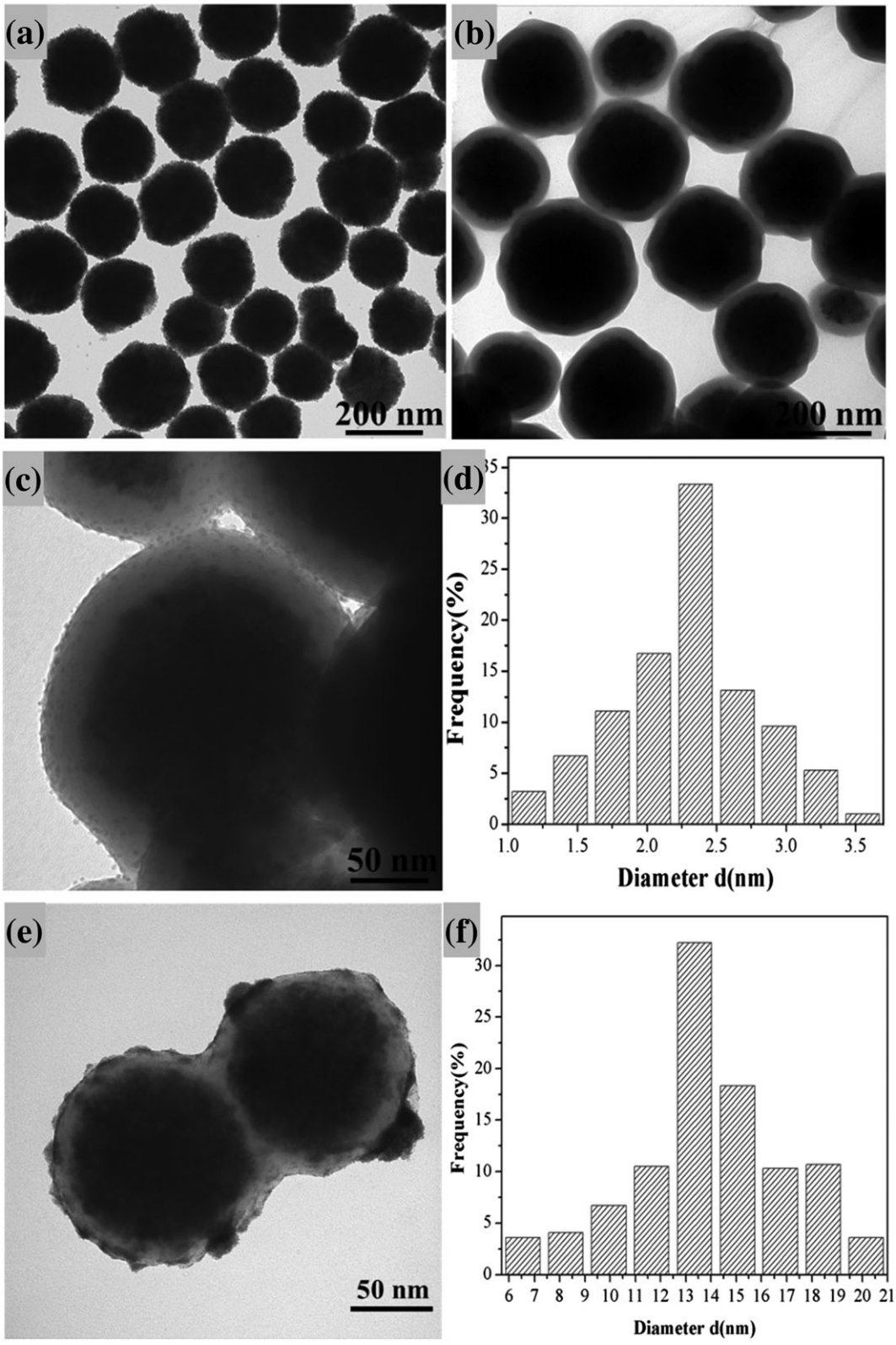

FIGURE 2 TEM images of Fe_3O_4 (a), Fe_3O_4@SiO_2 (b) and Fe_3O_4@SiO_2/APTS/Ru (c), and Ru particle distribution (d). TEM image of Fe_3O_4@SiO_2/Ru (e), and Ru particle distribution (f)

Figure 2 shows transmission electron microscopy (TEM) images of Fe_3O_4, Fe_3O_4@SiO_2 and Fe_3O_4@SiO_2/APTS/Ru, as well as the particle distributions of Ru. It is easily observed in Figure 2a that the diameter of the Fe_3O_4 particles was *ca* 270 nm with a narrow size distribution. As shown in Figure 2b, the core–shell structure of Fe_3O_4@SiO_2 can be clearly seen, with a uniform silica shell deposited on the Fe_3O_4 particles with a thickness of *ca* 28 nm. As illustrated in Figure 2c, numerous monodispersed Ru nanoparticles (2.5 nm) were uniformly decorated on the surface of Fe_3O_4@SiO_2, which was mainly due to the amino groups effectively preventing the aggregation of the Ru nanoparticles, ensuring that the Ru nanoparticles were not easily lost when reused in liquid-phase catalytic reactions.[31] Figure 2e shows that when no affinity ligands were used, although many of the Ru nanoparticles were located on the Fe_3O_4@SiO_2 particle surface, some major aggregates of Ru nanoparticles were also obviously observed on the surface of Fe_3O_4@SiO_2.

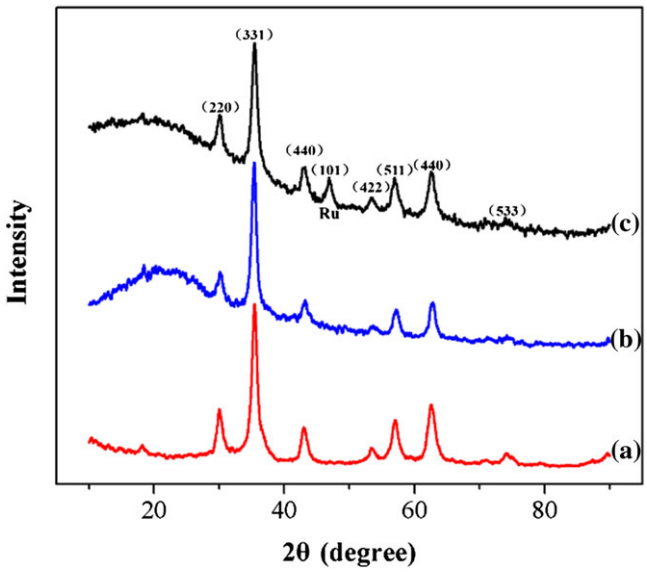

FIGURE 3 XRD patterns of Fe_3O_4 (a), Fe_3O_4@SiO_2 (b) and Fe_3O_4@SiO_2/APTS/Ru (c)

The crystallinity and phase composition of the resulting products were investigated using powder X-ray diffraction (XRD). Figure 3 displays the wide-angle XRD patterns of the samples. As shown in Figure 3a, all the peaks were in agreement with the face-centered cubic structure of Fe_3O_4. The diffraction peaks of Fe_3O_4 can be indexed to cubic Fe_3O_4 (JCPDS: 65-3107). After coating with SiO_2, a new broad peak at *ca* 23° appeared because of the existence of amorphous silica. For the Fe_3O_4@SiO_2/APTS/Ru samples, in addition to the Fe_3O_4 diffraction peaks, a tiny peak at 44° was distinguishable, owing to the characteristic diffraction of Ru(0). The XRD results indicated that the Ru nanoparticles had been successfully loaded onto the surface of the Fe_3O_4@SiO_2/APTS microspheres. The average size of the Ru crystallites, calculated using the Scherrer equation, was *ca* 2.5 nm, in good agreement with the average particle size derived from TEM analysis.[32]

To better understand the composition of Fe_3O_4@SiO_2/APTS/Ru, we carried out X-ray photoelectron spectroscopy (XPS) analysis. Figure 4 shows the XPS spectra of the surface of the Fe_3O_4@SiO_2/APTS/Ru. In Figure 4, the Ru binding energy of Fe_3O_4@SiO_2/APTS/Ru exhibited three strong peaks centered at 280.2, 461.5 and 484.5 eV, which were assigned to Ru $3d_{5/2}$, Ru $3p_{3/2}$ and Ru $3p_{1/2}$, respectively. The results from XPS revealed that Ru(0) existed in its elementary state. This was consistent with the XRD results.[33]

The magnetic properties of Fe_3O_4, Fe_3O_4@SiO_2 and Fe_3O_4@SiO_2/APTS/Ru nanoparticles were investigated using a vibrating sample magnetometer. The results are shown in Figure 5. All samples showed hysteresis loops without any detectable remanence, reflecting the superparamagnetic properties of the samples. The saturation magnetization values of Fe_3O_4@SiO_2 and

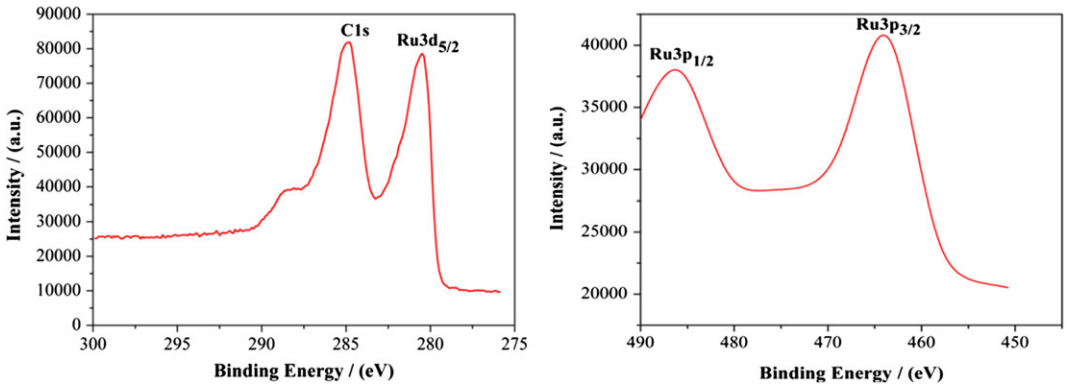

FIGURE 4 XPS spectra of Fe_3O_4@SiO_2/APTS/Ru

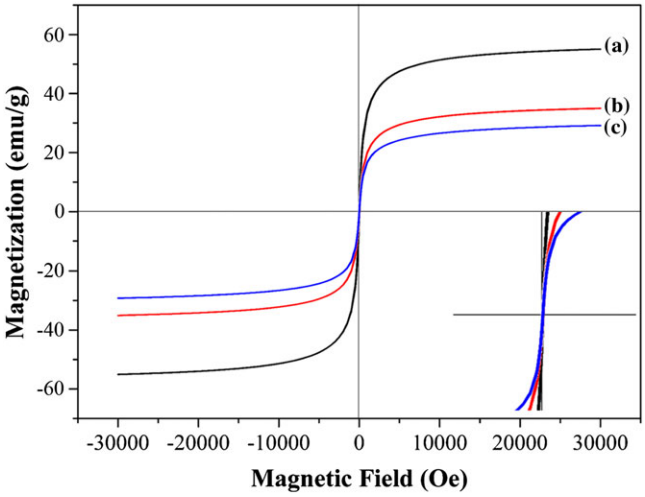

FIGURE 5 Magnetization curves of Fe_3O_4 (a), Fe_3O_4@SiO_2 (b) and Fe_3O_4@SiO_2/APTS/Ru (c)

Fe_3O_4@SiO_2/APTS/Ru were 43.6 and 41.1 emu g^{-1}, respectively. The decrease in the saturation magnetization suggested the presence of some Ru particles on the surface of the magnetic supports. Even with this reduction in the saturation magnetization, the catalyst was still efficiently and easily separated from solution with the help of an external magnetic force. As a result of the superparamagnetic properties and high magnetization, the Fe_3O_4@SiO_2/APTS/Ru nanoparticles showed fast separation under an applied magnetic field and quick dispersion through a slight shake when the magnetic field was removed.

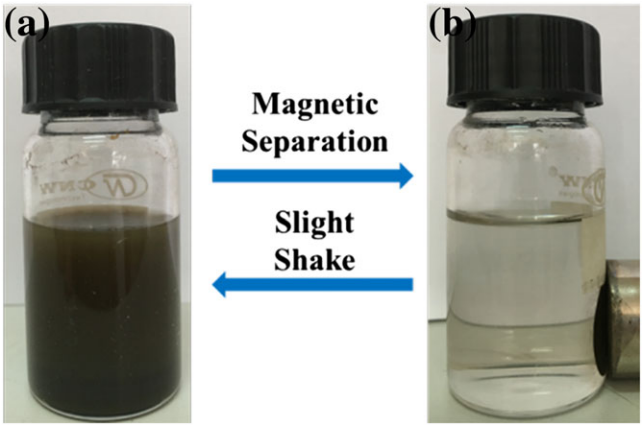

FIGURE 6 Photographs of catalyst dispersed in reaction mixture (a) and magnetic separation of catalyst from reaction medium (b)

2.2 | Catalyst testing for hydrogenation reactions

Here, we chose the hydrogenation of a variety of aromatic nitro compounds as a model to further study the

TABLE 1 Hydrogenation of various substrates catalyzed by Fe_3O_4@SiO_2/APTS/Ru[a]

Entry	Substrate	Product	Time (min)	Yield (%)	TOF (h^{-1})	TON
1	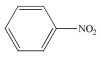	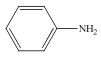	40	>99 >99[b] 96[c] 86[d]	198 197 192 174	131 131 128 116
2	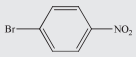		40	95	190	127
3	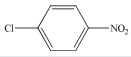	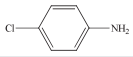	40	>99	196	130
4			40	98	196	130
5	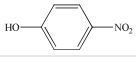		40	>99	197	131
6	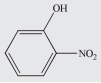	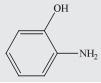	40	>99	198	131
7	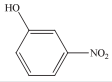	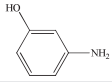	40	>99	197	131
8	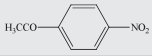	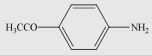	40	98	196	130

[a]Reaction conditions: Fe_3O_4@SiO_2/APTS/Ru, 0.05 g; loading of metal nanoparticles, 10 wt%; H_2, 1 atm; room temperature; substrate, 5.0 mmol; solvent, 5 ml.

[b]Yield after five runs.

[c]Hydrogenation with 10% Ru/C; the amount of catalysts was decided according to the same metal loading.

[d]Yield after five runs catalyzed by Ru/C.

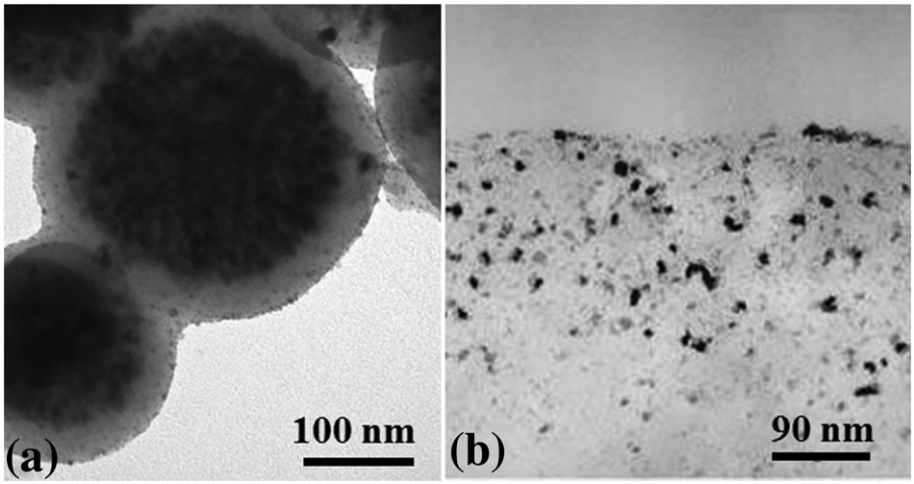

FIGURE 7 TEM images of Fe_3O_4@SiO_2/APTS/Ru (a) and Ru/C (b) after five runs of hydrogenation

performance of the Fe_3O_4@SiO_2/APTS/Ru nanospheres (S1). The reactions were carried out in ethanol at room temperature and under 1 atm of H_2. As evident from Table 1, we observed that the catalyst was very active for the hydrogenation reaction under mild conditions. The catalytic hydrogenation of aromatic nitro compounds produced yields of over 95%. In contrast, commercial 10% Ru/C was used to catalyze the hydrogenation reaction of nitrobenzene. The first yield was equal to that for Fe_3O_4@SiO_2/APTS/Ru. The good catalytic activity of the Fe_3O_4@SiO_2/APTS/Ru nanospheres was derived from their ultra-small sizes and highly dispersed Ru nanoparticles. The ultra-small sizes and highly dispersed Ru nanoparticles resulted in a high specific surface area, allowing the aromatic nitro compound ions to easily access the Ru nanoparticles that serve as an electron relay in the system for a reductant, thus leading to a high rate of reduction.[34] Furthermore, the reusability of Fe_3O_4@SiO_2/APTS/Ru was assessed in catalyzing the hydrogenation of nitrobenzene. After completion of the reaction, the catalyst was recovered in a facile manner from the reaction mixture using a permanent magnet (Figure 6). A satisfactory yield (>99%) was still obtained even after the catalyst had been reused five times, the nitrobenzene conversion being 99.7% and the aniline selectivity 99.3%. The good reusability of Fe_3O_4@SiO_2/APTS/Ru was attributed to the strong stability of the Ru nanoparticles on Fe_3O_4@SiO_2/APTS, which originates from the presence of multiple amino functional groups on the Fe_3O_4@SiO_2/APTS shell, and to the very limited loss of the Ru nanoparticles. The loading of the amino groups in the catalyst was 2.1%, determined through the XPS characterization technique. After the fifth reaction cycle, the loading of the amino groups was 2.0%, nearly no loss of amino groups. In addition, the catalyst was completely separated by applying an external magnetic field. No appreciable Ru leaching into the organic phase was observed after the fifth reaction cycle, as indicated by the inductively coupled plasma atomic emission spectrometry (ICP-AES) analysis result of 0.79 ppm. The TEM image (Figure 7a) of the catalyst obtained after the fifth cycle of the reaction did not show a significant change in catalyst morphology. The Ru nanoparticles remained highly dispersed on Fe_3O_4@SiO_2/APTS with an average size of 3.2 ± 0.5 nm. In our study, APTS might have served as a strong affinity ligand for high Ru dispersion, effectively preventing the agglomeration of Ru nanoparticles during the reaction.

For comparison, Ru/C was also separated by centrifuging and recycling in the hydrogenation reaction. The Ru content adopted during the recycling experiments in the mixed solution was kept the same for both the Ru/C catalyst and the Fe_3O_4@SiO_2/APTS/Ru composite microspheres. As clearly evident from Table 1, the yield after five runs using Ru/C was only 86%, the nitrobenzene conversion was 88.1% and the aniline selectivity was 97.6%. This result was probably due to the aggregation of the Ru nanoparticles, which might have happened after each cycle (Figure 7b). In addition, the Ru content in the catalyst was significantly reduced according to ICP-AES analysis, from 7.6 to 3.1%, indicating that the active components were lost during the cycling. Thus, the surface area of the catalyst, as well as the catalytic sites, decreased.

3 | CONCLUSIONS

An amino-modified core–shell structure catalyst nanocomposite, Fe_3O_4@SiO_2/APTS/Ru, was prepared. Ru

nanoparticles were not only ultra-small with nearly monodisperse sizes but also had a strong affinity with the surface of amino-functionalized Fe_3O_4@SiO_2. Amino groups effectively immobilized the Ru nanoparticles, promoting their single dispersion and preventing them from aggregating, meaning Fe_3O_4@SiO_2/APTS/Ru exhibited good reusability. The obtained catalyst exhibited excellent catalytic performance for the hydrogenation of a variety of aromatic nitro compounds, even at room temperature, giving yields of over 95%. Furthermore, Fe_3O_4@SiO_2/APTS/Ru was easily recovered using a magnetic field and directly reused for at least five cycles without significant loss of its activity.

ACKNOWLEDGEMENTS

This work was financially supported by the Taishan Scholars Projects of Shandong (ts201511033), the National Natural Science Foundation of China (31700517), the Open Fund of the Biomass-energy and Materials Key Laboratory of Jiangsu (JSBEM201802), the Key R&D project of Shandong (2017GGX70102), 13th National 5-year R&D plans in rural areas (2016YFD0600804). The authors are grateful for the financial support.

CONFLICT OF INTEREST

The authors declare that they have no conflict of interest.

Compliance with ethical standards

ORCID

Yue Liu https://orcid.org/0000-0002-2663-6133

REFERENCES

[1] S. Neretina, R. A. Hughes, K. D. Gilroy, M. Hajfathalian, *Acc. Chem. Res.* **2016**, *49*, 2243.

[2] W. Liu, A. K. Herrmann, N. C. Bigall, P. Rodriguez, D. Wen, M. Oezaslan, T. J. Schmidt, N. Gaponik, A. Eychmller, *Acc. Chem. Res.* **2015**, *48*, 154.

[3] K. M. Choi, K. Na, G. A. Somorjai, O. M. Yaghi, *J. Am. Chem. Soc.* **2015**, *137*, 7810.

[4] T. Kim, X. Fu, D. Warther, M. J. Sailor, *ACS Nano* **2017**, *11*, 2773.

[5] A. Dhakshinamoorthy, A. M. Asiri, H. Garcia, *ACS Catal.* **2017**, *7*, 2896.

[6] J. H. Koo, S. W. Lee, J. Y. Park, I. S. Lee, *Chem. Mater.* **2017**, *29*, 9463.

[7] Y. Li, C. Jin, G. Yuan, J. Han, M. Wang, R. Guo, *Langmuir* **2017**, *33*, 7486.

[8] Z. J. Wang, S. Ghasimi, K. Landfester, K. A. I. Zhang, *Chem. Mater.* **2015**, *27*, 1921.

[9] Y. Chen, Q. L. Zhu, N. Tsumori, Q. Xu, *J. Am. Chem. Soc.* **2015**, *137*, 106.

[10] Z. Dong, X. Le, C. Dong, W. Zhang, X. Li, J. Ma, *Appl. Catal. B* **2015**, *162*, 372.

[11] J. Chen, J. Wang, J. Chen, L. Wang, *J. Mater. Sci.* **2017**, *52*, 13064.

[12] M. Zhao, K. Deng, L. He, Y. Liu, G. Li, H. Zhao, Z. Tang, *J. Am. Chem. Soc.* **2014**, *136*, 1738.

[13] W. Li, X. Yue, C. Guo, J. P. Lv, S. S. Liu, Y. Zhang, J. Xu, *Appl. Surf. Sci.* **2015**, *335*, 23.

[14] E. Murugan, J. N. Jebaranjitham, *Chem. Eng. J.* **2015**, *259*, 266.

[15] M. Kiani, M. Mohammadipour, *RSC Adv.* **2017**, *7*, 997.

[16] Y. Liu, N. Cherkasov, P. Gao, J. Fernández, M. R. Lees, E. V. Rebrov, *J. Catal.* **2017**, *355*, 120.

[17] C. Nadejde, M. Neamtu, V. D. Hodoroaba, R. J. Schneider, G. Ababei, U. Panne, *Chem. Eng. J.* **2016**, *302*, 587.

[18] P. Lisk, E. Bonnot, M. T. Rahman, R. Pollard, R. Bowman, V. Degirmenci, E. V. Rebrov, *Chem. Eng. J.* **2016**, *306*, 352.

[19] T. Feng, X. Qiao, H. Wang, Z. Sun, C. Hong, *Biosens. Bioelectron.* **2016**, *79*, 48.

[20] H. Guan, C. Chao, W. Kong, Z. Hu, Y. Zhao, S. Yuan, B. Zhang, *J. Nanopart. Res.* **2017**, *19*, 187.

[21] P. Panja, P. Das, K. Mandal, N. R. Jana, *ACS Sustain. Chem. Eng.* **2017**, *5*, 4879.

[22] Y. Zhang, F. Gao, B. Wanjala, Z. Li, G. Cernigliaro, Z. Gu, *Appl. Catal. B* **2016**, *199*, 504.

[23] S. Rostamnia, B. Gholipour, X. Liu, Y. Wang, H. Arandiyan, *J. Colloid Interface Sci.* **2018**, *511*, 447.

[24] M. Dehghan, A. Motaharinejad, M. Saadat, R. Ahdenov, M. Babazadeh, R. Hosseinzadeh-Khanmiri, *RSC Adv.* **2015**, *5*, 92335.

[25] E. Soleimani, N. Yaesoobi, H. R. Ghasempour, *Appl. Organometal. Chem.* **2018**, *32*, e4006.

[26] A. S. Piskun, J. Ftouni, Z. Tang, B. M. Weckhuysen, P. C. A. Bruijnincx, H. J. Heeres, *Appl. Catal. A* **2018**, *549*, 197.

[27] K. Rohmann, J. Kothe, M. W. Haenel, U. Englert, M. Hölscher, W. Leitner, *Angew. Chem. Int. Edit.* **2016**, *55*, 8966.

[28] D. V. Arulmani, J. I. Eastcott, S. G. Mavilla, E. B. Easton, *J. Power Sources* **2014**, *247*, 890.

[29] F. Wang, S. He, H. Chen, B. Wang, L. Zheng, M. Wei, D. G. Evans, X. Duan, *J. Am. Chem. Soc.* **2016**, *138*, 6298.

[30] Y. Deng, Y. Cai, Z. Sun, J. Liu, C. Liu, J. Wei, W. Li, C. Liu, Y. Wang, D. Zhao, *J. Am. Chem. Soc.* **2010**, *132*, 8466.

[31] M. Guo, G. Lan, J. Peng, M. Li, Q. Yang, C. Li, *J. Mater. Chem. A* **2016**, *4*, 10956.

[32] B. Lin, C. Xue, X. Yan, G. Yang, G. Yang, B. Yang, *Appl. Surf. Sci.* **2015**, *357*, 346.

[33] M. Sudhakar, V. V. Kumar, G. Naresh, M. L. Kantam, S. K. Bhargava, A. Venugopal, *Appl. Catal. B* **2016**, *180*, 113.

[34] Y. Chi, J. Tu, M. Wang, X. Li, Z. Zhao, *J. Colloid Interface Sci.* **2014**, *423*, 54.

SUPPORTING INFORMATION

Additional supporting information may be found online in the Supporting Information section at the end of the article.

How to cite this article: Liu Y, Lv M, Li L, et al. Synthesis of a highly active amino-functionalized Fe_3O_4@SiO_2/APTS/Ru magnetic nanocomposite catalyst for hydrogenation reactions. *Appl Organometal Chem*. 2019;e4686. https://doi.org/10.1002/aoc.4686